Phage mobility is a core determinant of phage-bacteria coexistence in biofilms

Running title: Phage diffusion in bacterial biofilms

Matthew Simmons[1], Knut Drescher[2,3], Carey D. Nadell[2,4]*†, Vanni Bucci[1]*†

[1] Department of Biology, Program in Biotechnology and Biomedical Engineering, University of Massachusetts Dartmouth, N. Dartmouth, MA 02747, USA

[2] Max Planck Institute for Terrestrial Microbiology, D-35043 Marburg, Germany

[3] Department of Physics, Philipps University Marburg, D-35032 Marburg, Germany

[4] Current Address: Department of Biological Sciences, Dartmouth College, Hanover, NH 03755, USA

*** Equal contribution**

† **Correspondence to:** Carey.D.Nadell@dartmouth.edu, vanni.bucci@umassd.edu

Abstract

Many bacteria are adapted for attaching to surfaces and for building complex communities, termed biofilms. The biofilm mode of life is predominant in bacterial ecology. So, too, is exposure of bacteria to ubiquitous viral pathogens, termed bacteriophages. Although biofilm-phage encounters are likely to be very common in nature, little is known about how phages might interact with biofilm-dwelling bacteria. It is also unclear how the ecological dynamics of phages and their hosts depend on the biological and physical properties of the biofilm environment. To make headway in this area, here we develop the first biofilm simulation framework that captures key features of biofilm growth and phage infection. Using these simulations, we find that the equilibrium state of interaction between biofilms and phages is governed largely by nutrient availability to biofilms, phage infection likelihood, and the ability of phages to diffuse through biofilm populations. Interactions between the biofilm matrix and phage particles are thus likely to be of fundamental importance, controlling the extent to which bacteria and phages can coexist in natural contexts. Our results open avenues to new questions of host-parasite coevolution in the spatially structured biofilm context.

Keywords

biofilm, phage, phage mobility, diffusion limitation, matrix, host-parasite, simulation, spatial structure

Introduction

Bacteriophages, the viral parasites of bacteria, are predominant agents of bacterial death in nature [1]. Their ecological importance and relative ease of culture in the lab have made bacteria and their phages a centerpiece of classical and recent studies of molecular genetics [2-6] and host-parasite coevolution [7-17]. This is a venerable literature with many landmark discoveries, the majority of which have focused on bacteria-phage interaction in liquid culture. In addition to living in the planktonic phase, many microbes are adapted for interacting with surfaces, attaching to them, and forming multicellular communities [18-23]. These communities, termed biofilms, are characteristically embedded in an extracellular matrix of proteins, DNA, and sugar polymers that play a large role in how the community interacts with the surrounding environment.

Since growth in biofilms and exposure to phages are common features of bacterial life, we can expect biofilm-phage encounters to be fundamental to microbial natural history [24-29]. Furthermore, using phages as a means to kill unwanted bacteria – which was eclipsed in 1940 by the advent of antibiotics in Western medicine – has experienced a revival in recent years as an alternative antimicrobial strategy [30-35]. Understanding biofilm-phage interactions is thus an important new direction for molecular, ecological, and applied microbiology. Existing work suggests that phage particles may be trapped in the extracellular matrix of biofilms [36-38]; other studies have used macroscopic staining assays to measure changes in biofilm size before and after phage exposure, with results ranging from biofilm death, to no effect, to biofilm augmentation [39]. There is currently only a very limited understanding of the mechanisms responsible for this observed variation in outcome, and there has been no systematic exploration of how phage infections spread within living biofilms on the length scales of bacterial cells.

Biofilms, even when derived from a single clone, are heterogeneous in space and time [40, 41]. The extracellular matrix can immobilize a large fraction of cells, constraining their movement and the mass transport of soluble nutrients and wastes [20, 42]. Population spatial structure is of fundamental importance due to its impact on intra- and inter-specific interaction patterns [43, 44]. Furthermore, epidemiological theory predicts qualitative changes in population dynamics when host-parasite contact rate is not a simple linear function of host and parasite abundance [45], which is certainly the case for phages and biofilm-dwelling bacteria under spatial constraint. It is thus very likely that the interaction of bacteria and phages will be altered in biofilms relative to mixed or stationary liquid environments. This alteration could manifest owing to differences in phage diffusivity within biofilms, physical shielding of internal host populations by peripheral cells, differential speed of bacterial division versus phage proliferation, or other features of the biofilm mode of growth. Available literature supports the possibility of altered phage population dynamics in biofilms [14, 15, 46-48], but the underlying details of the phage-bacterial interactions have been difficult to access experimentally or theoretically.

Existing biofilm simulation frameworks are flexible and have excellent experimental support [49-54], but they become impractical when applied to the problem of phage infection [55]. We therefore developed a novel approach to study phage-biofilm interactions *via* spatially explicit simulations. We applied this new framework to explore population dynamics in a minimal system containing lytic phages and susceptible host cells. We find that nutrient availability and phage infection rates are critical control parameters of phage spread; furthermore, modest changes in the diffusivity of phages within biofilms can cause qualitative shifts toward stable or unstable coexistence of phages and biofilm-dwelling bacteria. The latter result implies a central role for the biofilm extracellular matrix in phage ecology, as it could significantly modify phage diffusion. A full understanding of the interactions between bacteria and their phages therefore requires explicit consideration of the biofilm mode of bacterial life.

Methods

When phages are implemented as discrete individuals, the total number of independent agents in a single simulation on spatial scales of hundreds of bacterial cell lengths can rapidly reach many hundreds of thousands. Moreover, the time scale for calculating bacterial growth can be an order of magnitude larger than the appropriate time scale for phage replication and diffusion. These computational challenges limit the use of traditional biofilm simulations for studying phage infection [55, 56], and we therefore developed a new framework customized for biofilm-phage interactions. Our model combines (*i*) a numerical solution of partial differential equations to determine solute concentrations in space, (*ii*) a cellular automaton method for simulating biofilms containing a user-defined, arbitrary number of bacterial strains with potentially different properties, and (*iii*) an agent-based method for simulating diffusible phages (Figure 1).

The methods developed here are motivated by a well-developed and empirically supported family of biofilm simulation frameworks [50, 54, 55, 57], but with the addition of special modifications for implementing phage replication and diffusion. In the present study, we restrict ourselves to two-dimensional simulation spaces. In each simulation run, the simulation space (250 μm x 250 μm) is initiated with cells that are randomly distributed across the basal surface. The following steps are iterated until an exit steady-state criterion is met:

– Compute nutrient concentration profiles
– Compute bacterial biomass dynamics
– Redistribute biomass according to cellular automaton rules (i.e., cell shoving)
– Evaluate host cell lysis and phage propagation
– Simulate phage diffusion to determine new distribution of phage particles
– Assessment of match to exit criteria:
  Coexistence: simulations reach a pre-defined end time with both bacteria and phages still present (these cases are re-assessed for long-term stability);
  Biofilm death: the bacterial population declines to zero; or
  Phage extinction: no phages or infected biomass remain in the biofilm.

As in previous biofilm simulation frameworks, bacteria grow and divide according to local nutrient concentrations, which are calculated to account for diffusion from a bulk nutrient supply and absorption by bacteria. Specifically, when nutrients are abundant, most cells in the biofilm can grow. When nutrients are scarce, they are depleted by cells on the outermost layers of the biofilm, and bacteria in the interior stop growing. Cells on the exterior of the biofilm can be eroded due to shear [58-61]. Implementing biomass removal by shear is critical in allowing us to study the long-term steady states of the system: without shear-induced sloughing, one is restricted to examining transient biofilm states [57, 62]. Furthermore, biofilm sloughing is critical to implementing loss of biofilm biomass when phage infections destroy biofilms with rough surface fronts (see below). Bacterial growth, decay, and shear are implemented according to supported precedents in the literature [62-65].

Implementing phage infection, propagation, and diffusion is the primary innovation of the simulation framework we developed. To mimic phages that encounter a pre-grown biofilm after departing from a previous infection site, we performed our simulations such that biofilms could grow for a defined period, after which a single pulse of phages was introduced into the simulation space. During this pulse, lytic phages [24] are added to the simulation space all along the biofilm front. For every phage virion located in a grid-cell containing bacterial biomass, we calculate the probability of adsorption to a bacterial cell, which is a function of the infection rate and the number of susceptible hosts available in the particular grid-cell. Upon adsorption, the corresponding bacterial biomass is converted from uninfected to an infected state (Figure 1). Following an incubation period, the host cell lyses and releases progeny phages with a defined burst size. Here the burst size is fixed at an empirically conservative number, but we explore variation in burst size in a supplementary analysis (see below). Phages move within the biofilm and in the liquid medium by Brownian motion; the model analytically solves the diffusion equation of a Dirac delta function at each grid cell to build a probability distribution from which to resample the phage locations.

The way in which phages diffuse is likely to be important for how phage-biofilm interactions occur, and we devoted particular attention to building flexibility into the framework for this purpose. The diffusivity of phage particles is likely to decrease when they are embedded in biofilm matrix material, but the extent to which their movement is affected is not well understood. To study how phage movement inside biofilms influences phage infection dynamics, we introduce a parameter, Z_p, which we term phage impedance. For $Z_p = 1$, phage diffusivity is the same inside and outside of biofilms. As the value of Z_p is increased, phage diffusive movement inside biofilms is decreased relative to normal aqueous solutions. Furthermore, theory predicts that it will be easier for a diffusing particle to enter a 3-dimensional mesh maze, as one can consider the biofilm matrix, than it is for the same particle to exit the mesh [66, 67]. Our model of phage movement incorporates this predicted property of biofilm matrix material by making it easier for phages to cross from the surrounding liquid to the biofilm mass fraction than *vice versa* (see SI Text). We also explore the consequences of relaxing this assumption, such that phages can cross from the surrounding liquid to biofilm, and *vice versa*, with equal ease.

All model parameters, where possible, were set according to precedent in the experimental and biofilm simulation literature (see Table 1). To test the core dynamics of our framework, we compared the predictions obtained from the framework (using well-mixed nutrient, bacterial, and phage distributions) with results obtained from an ODE model incorporating the same processes and parameters as the simulations. These trials confirmed that the core population dynamics of the simulations perform according to expectation without spatial structure (see SI Text and Supplementary Figure S1). A detailed description of the simulation framework and explanation of its assumptions are provided in the Supplementary Material**.** The framework code can be obtained from the Zenodo repository: https://zenodo.org/record/268903#.WJho3bYrJHc.

Computation

Our hybrid framework was written in the Python programming language, drawing from numerical methods developed in the literature [68-70]. All data analysis was performed using the R programming language (see Supplementary Data). Simulations were performed *en mass* in parallel on the UMass Green High Performance Computing Cluster. Each simulation requires 4-8 hours to run, and more than 150,000 simulations were performed for this study, totaling over 100 CPU-years of computing time.

Results

A primary feature distinguishing biofilm populations from planktonic populations is spatial constraint and heterogeneity in the distribution of solutes, cell growth, and – we hypothesize – phage infection. Thus our goal in this study is to identify key parameter sets that influence phage-biofilm interactions, with particular focus on variable phage transport through biofilms. We began by exploring the different possible outcomes of phage infection and biofilms as a function of phage infectivity, before moving on to a more systematic study of phage transport, phage infection, and bacterial growth rates.

(a) Stable states of bacteria and phages in biofilms

Intuitively, the population dynamics of bacteria and lytic phages should depend on the relative strength of bacterial growth and bacterial removal, including erosion and cell death caused by phage infection and proliferation. We studied the behavior of the simulation by varying the relative magnitude of bacterial growth versus phage proliferation. In this manner, we could observe three broad stable state classes in the bacteria/phage population dynamics (Figure 2). We summarize these classes here before proceeding to a more systematic characterization of the simulation parameter space in the following section.

(i) Biofilm death

If phage infection and proliferation sufficiently out-pace bacterial growth, then the bacterial population eventually declines to zero as it is consumed by phages and erosion (Figure 2A).

Phage infections progressed in a relatively homogeneous wave, if host biofilms were flat (Supplementary Video SV1). For biofilms with uneven surface topography, phage infections proceeded tangentially to the biofilm surface and "pinched off" areas of bacterial biomass, which were then sloughed away after losing their connection to the remainder of the biofilm (Supplementary Video SV2). This sloughing process eventually eliminated the bacterial population from the surface.

(ii) Coexistence

In some instances, both bacteria and phages remained present for the entire simulation run time. We found that coexistence could occur in different ways, most commonly with rounded biofilm clusters that were maintained by a balance of bacterial growth and death on their periphery (Supplementary Video SV3). When phage infection rate and nutrient availability were high, biofilms entered cycles in which tower structures were pinched off from the rest of the population by phage propagation, and from the remaining biofilm, new tower structures re-grew and were again partially removed by phages (Figure 2B and Supplementary Video SV4). We confirmed the stability of these coexistence outcomes by running simulations for extended periods of time, varying initial conditions and the timing of phage exposure to ensure that host and phage population sizes either approached constant values or entrained in oscillation regimes (see below).

(iii) Phage extinction

We observed many cases in which phages either failed to establish a spreading infection, or declined to extinction after briefly propagating in the biofilm (Figure 2C). This occurred when phage infection probability was low, but also, less intuitively, when nutrient availability and thus bacterial growth were very low, irrespective of infection probability. Visual inspection of the simulations showed that when biofilms were sparse and slow-growing, newly released phages were more likely to be swept away into the liquid phase than to encounter new host cells to infect (Supplementary Video SV5). At a conservative maximum bacterial growth rate, biofilms were not able to out-grow a phage infection. However, if bacterial growth was increased beyond this conservative maximum, we found that biofilms could effectively expel phage infections by shedding phages into the liquid phase above them (Supplementary Video SV6). This result, and those described above, heavily depended on the ability of phages to diffuse through the biofilms, to which we turn our attention in the following section.

(b) Governing parameters of phage spread in biofilms

Many processes can contribute to the balance of bacterial growth and phage propagation in a biofilm [71, 72]. To probe our simulation framework systematically, we first chose control parameters with strong influence on the outcome of phage-host population dynamics. We then performed sweeps of parameter space to build up a general picture of how the population dynamics of the biofilm-phage system depends on underlying features of phages, host bacteria, and biofilm spatial structure.

We isolated three key parameters with major effects on how phage infections spread through biofilms [48, 72, 73]. The first of these is environmental nutrient concentration, $N_{\max}$, an important ecological factor that heavily influences biofilm growth rate. Importantly, varying $N_{\max}$ not only changes the overall growth rate but also the emergent biofilm spatial structure [74, 75]. When nutrients are sparse, for example, biofilms grow with tower-like projections and high variance in surface height [76], whereas when nutrients are abundant, biofilms tend to grow with smooth fronts and low variance in surface height [72, 74, 76]. We computationally swept $N_{\max}$ values to vary biofilm growth from near zero to a conservative maximum allowing for biofilm growth to a height of 250 μm in 24 hours without phage exposure. The second governing parameter is phage infection probability, which we varied from 0.1% to 99% per phage-host encounter. Phage burst size is also important, but above a threshold value (approximately 100 new phages per lysed host), we found that its qualitative influence on our results saturated (Supplementary Figure S2). Lower burst sizes exerted similar effects to lowering the probability of phage infection per host encounter. Therefore, for simplicity in the

rest of the paper, we use a fixed burst size of 100, which is typical for model lytic phages such as T7 [77].

Our pilot simulations with the framework suggested that a third factor, the relative diffusivity of phages within biofilms, may be fundamental to phage-bacteria population dynamics. We therefore varied phage movement within the biofilm by changing the phage impedance parameter Z_P; larger values of Z_P correspond to slower phage diffusivity within biofilms relative to the surrounding liquid.

We performed thousands of simulations in parallel to study the influence of nutrients, infection probability, and phage mobility on population dynamics. All the other simulation parameters were fixed according to values taken from the experimental literature (see Table 1). In Figure 3, the results are visualized as sweeps of nutrient concentration versus phage infectivity for three values of phage impedance. For each combination of these three parameters, we show the distribution of simulation exit conditions, including biofilm death, phage extinction, or phage-bacteria coexistence. In some cases, biofilms grew to the ceiling of the simulation space, such that the biofilm front could no longer be simulated accurately. To be conservative, the outcome of these cases was designated as "undetermined", but they likely correspond to phage extinction or phage-bacteria coexistence.

We first considered the extreme case in which phage diffusion is unaltered inside biofilms (phage impedance value of Z_p = 1). In these conditions, coexistence does not occur, and bacterial populations do not survive phage exposure unless infection probability is nearly zero, or if nutrient availability is so low that little bacterial growth is possible. In these latter cases, as we described above, phages either cannot establish an infection at all or are unlikely to encounter new hosts after departing from an infected host after it bursts. Interestingly, bacterial survival in this regime depends on the spatial structure of biofilm growth, including the assumption that phages which have diffused away from the biofilm surface are advected out of the system. Importantly, using the same experimentally constrained parameters for bacteria and phages, but in a spatially homogenized version of the framework – which approximates a mixed liquid condition – total elimination of the bacterial population was the only outcome (Supplementary Figure S1). This comparison further highlights the importance of spatial effects on this system's ecological dynamics.

When phage diffusivity is reduced within biofilms relative to the surrounding liquid (phage impedance value of Z_P = 10), biofilm-dwelling bacteria survive infection for a wider range of phage infection probability (Figure 3b). Phages and host bacteria coexist with each other at low to moderate infection probability and high nutrient availability for bacterial growth. Within this region of coexistence, we could find cases where phage and host populations converge to stable fixed equilibria, and others in which bacterial and phage populations enter stable oscillations. The former corresponds to stationary biofilm clusters with a balance of bacterial growth and phage proliferation on their periphery (as in Supplementary Video SV3), while the latter corresponds to cycles of biofilm tower projection growth and sloughing after phage proliferation (as in Supplementary Video SV4). For low nutrient availability, slow-growing biofilms could avoid phage epidemics by providing too few host cells for continuing infection.

As phage diffusivity within biofilms is decreased further (Figure 3c), coexistence occurs for a broader range of nutrient and infectivity conditions, and biofilm-dwelling bacteria are more likely to survive phage exposure. Interestingly, for Z_P = 15 there was a substantial expansion of the parameter range in which biofilms survive and phages go extinct. For Z_P = 10 and Z_P = 15, we also found cases of unstable coexistence in which bacteria and phages persisted together transiently, but then either the host or the phage population declined to extinction stochastically over time (Figure 3d-e). Depending on the relative magnitudes of bacterial growth (low vs. high nutrients) and phage infection rates, this unstable coexistence regime was shifted toward biofilm survival or phage extinction in the long run.

The stochasticity inherent to the spatial simulations provides an inherent test of stability to small perturbations. In order to assess the broader robustness of our results to initial conditions, we repeated the parameter sweeps, but varied the time at which phages were introduced. We found that the outcomes were qualitatively identical when compared with the data described above (Supplementary Figure S3).

Overall, the landscape of different system stable states in parameter space can be quite complex. For example, in Figure 3E-F, at intermediate phage infectivity, low nutrient availability resulted in biofilm survival. Increasing nutrient input leads to biofilm death as biofilms become large enough for phages to take hold and spread through the population. Further increasing nutrient availability leads to a region of predominant coexistence as higher bacterial growth compensates for phage-mediated death. And, finally, increasing nutrient input further still leads to stochastic outcomes of biofilm survival and biofilm death, with the degree of biofilm sloughing and erosion imposing chance effects on whether biofilms survive phage exposure.

(c) Population stable states as a function of phage diffusivity

The findings summarized in Figure 3 suggest that phage diffusivity (reflected by the phage impedance Z_p) is a critical parameter controlling population dynamics in biofilms. We assessed this idea systemically by varying phage impedance at high resolution and determining the effects on phage/bacteria stable states spectra within biofilms. For each value of phage impedance ($Z_P = 1 - 18$), we performed parameter sweeps for the same range of nutrient availability and phage infection probability as described in the previous section, and quantified the fraction of simulations resulting in biofilm death, phage-bacteria coexistence, and phage extinction (Figure 4). With increasing Z_P we found an increase in the fraction of simulations ending in long-term biofilm survival, either *via* phage extinction or *via* coexistence, and a corresponding decrease in conditions leading to biofilm extinction. We expected the parameter space in which phages eliminate biofilms to contract to nil as phage impedance was increased. However, this was not the case; the stable states distribution, which saturated at approximately $Z_P = 15$, always presented a fraction of simulations in which bacteria were eliminated by phages. This result depended to a degree on the symmetry of phage diffusion across the interface of the biofilm and the surrounding liquid. As noted in the Methods section, theory predicts that phages can enter the biofilm matrix mesh more easily than they can exit, and this is the default mode of our simulations. If, on the other hand, phages can diffuse across the biofilm boundary back into the liquid just as easily as they can cross from the liquid to the biofilm, then as Z_P increases, then biofilm death occurs less often, and bacteria-phage coexistence becomes the predominant state (Supplementary Figure S4).

Discussion

Biofilm-phage interactions are likely to be ubiquitous in the natural environment and, increasingly, phages are drawing attention as the basis for new antibacterial strategies [78]. Due to the complexity of the spatial interplay between bacteria and their phages in the biofilm context, simulations and mathematical modeling serve a critical role for identifying important features of phage-biofilm interactions. The biofilm mode of growth possesses numerous features that require specific treatment for modeling phage infections. For example, the interactions between nutrient gradients, cell proliferation, biofilm erosion, and phage movement all distinguish the biofilm environment from broader classes of agent based models for studying the spatial spread of disease [79-81]. We therefore developed a new simulation framework that captures these essential processes.

The interaction of bacterial growth, phage infection, and biofilm heterogeneity creates a rich landscape of different population dynamical behavior. At the outset of this work, we hypothesized that bacteria might be able to survive phage attack when nutrients are abundant and bacterial growth rate is high. The underlying rationale was that if bacterial growth and biofilm erosion are fast enough relative to Kovács phage proliferation, then biofilms could simply shed phage infections from their outer surface into the passing liquid. This result was not obtained when nutrient input and thus bacterial growth were set at conservatively high values. We speculate that in order for biofilms to shed phage infections in this manner, phage incubation times must be long in relation to bacterial growth rate, and/or biofilm erosion must be exceptionally strong, such that biomass on the biofilm exterior is rapidly and continuously lost into the liquid phase. Our results do not eliminate this possibility entirely, but they do suggest that this kind of spatial escape from phage infection does not occur under a broad range of conditions.

Biofilms were able to repel phage epidemics in our simulations when nutrient availability was low, resulting in slow bacterial growth and widely spaced biofilm clusters. When biofilms are sparse, phage-bacteria encounters are less likely to occur, and thus a higher probability of infection per phage-host contact event is required to establish a phage "epidemic". Even if phages do establish an infection in a biofilm cluster, when bacterial growth rates are low, the nearest biofilm cluster may be far enough away from the infected cluster that phages simply are not able to spread from one biofilm to another before being swept away by fluid flow. This result is directly analogous to the concept of threshold host density as it applies in wildlife disease ecology [79, 82-88]. If host organisms, or clusters of hosts, are not distributed densely enough relative to the production rate and dispersal of a parasite, then epidemics cannot be sustained. Note that in our system, this observation depends on the scale of observation [89]. In a meta-population context, phage proliferation and subsequent removal into the passing liquid may lead to an epidemic on a larger spatial scale, for example, if other areas are well populated by susceptible hosts.

Our simulations suggest that coexistence of lytic phages and susceptible host bacteria can occur more and more readily as the ability of phages to diffuse through biofilms decreases. In two important early papers on phage-bacteria interactions under spatial constraint, Heilmann et al. [48, 73] also suggested that coexistence occurs under a broad array of conditions as long as bacteria could produce refuges, that is, areas in which phage infectivity is decreased. An important distinction of our present work is that bacterial refuges against phage infection emerge spontaneously as a result of the interaction between biofilm growth, phage proliferation and diffusion, and erosion of biomass into the surrounding liquid phase. Furthermore, we emphasize that reducing phage infectivity and reducing phage diffusivity through biofilms are two alternative but complementary means by which biofilm-dwelling bacteria can enhance the chances for survival during phage exposure. Another important result of our simulations is that coexistence of biofilm-dwelling bacteria and lytic phages can be rendered dynamically unstable by modest changes in nutrient availability or phage infection likelihood. In these cases, the host bacterial population or the phages go extinct stochastically, with the balance between these two outcomes resting on the relative magnitudes of biofilm growth and phage infection probability.

The extracellular matrix is central to the ecology and physiological properties of biofilms [20, 42, 90-94]. In the simulations explored here, biofilm matrix was modeled implicitly and is assumed to cause changes in phage diffusivity; our results support the intuition that by altering phage mobility and their physical access to new hosts, the biofilm matrix is likely to be of fundamental importance in the ecological interplay of bacteria and their phages [95]. There is very little experimental work thus far on the spatial localization and diffusion of phages inside biofilms, but the available literature is consistent with the idea that the matrix interferes with phage movement [36, 37, 96]. Furthermore, experimental evolution work has shown that bacteria and their phages show different evolutionary trajectories in biofilms versus planktonic culture [15, 46, 97]. Especially notable here is the fact that *Pseudomonas fluorescens* evolves matrix hyper-production in response to consistent phage attack [46]. The molecular and ecological details by which the biofilm matrix influences phage proliferation are important areas for future study.

Here we have introduced a new approach to studying phage-biofilm interactions *in silico*, which required us to consider many unique features of bacterial growth in communities on surfaces. Using this framework, we have identified important parameters and spatial structures of biofilms that govern the population dynamics of phage infections. In light of these results, we envision that bacteria-phage coevolution in the biofilm context may present an important expansion upon the history of work on this classical area of microbial ecology.

Competing Interests

We have no competing interests.

Author Contributions

CDN and VB conceived the project; MS, VB, and CDN designed simulations; MS wrote and performed simulations and scripts for the raw figures; MS, CDN, VB, and KD analyzed data; CDN, VB, MS, and KD wrote the paper.

Acknowledgements

We are grateful to Ann Tate for comments on an early version of the manuscript. C.D.N. is supported by the Alexander von Humboldt Foundation. V.B. acknowledges support from the National Institute of Allergy and Infectious Disease (grant R15-AI112985-01A), and the National Science Foundation (grant 1458347). K.D. is supported by the Max Planck Society, the Human Frontier Science Program (CDA00084/2015-C), the Behrens Weise Foundation, and the European Research Council (716734).

References

[1] Suttle, C.A. 2007 Marine viruses—major players in the global ecosystem. *Nat Rev Microbiol* **5**, 801-812.

[2] Cairns, J., Stent, G.S. & Watson, J. 2007 *Phage and the Origins of Molecular Biology, Centennial Ed.* 2 ed. Plainview, NY, Cold Spring Harbor Laboratory Press.

[3] Salmond, G.P.C. & Fineran, P.C. 2015 A century of the phage: past, present and future. *Nat Rev Micro* **13**, 777-786. (doi:10.1038/nrmicro3564).

[4] Samson, J.E., Magadan, A.H., Sabri, M. & Moineau, S. 2013 Revenge of the phages: defeating bacterial defences. *Nat Rev Micro* **11**, 675-687. (doi:10.1038/nrmicro3096).

[5] Labrie, S.J., Samson, J.E. & Moineau, S. 2010 Bacteriophage resistance mechanisms. *Nat Rev Micro* **8**, 317-327.

[6] Susskind, M.M. & Botstein, D. 1978 Molecular genetics of bacteriophage P22. *Microbiological reviews* **42**, 385.

[7] Levin, B.R., Stewart, F.M. & Chao, L. 1977 Resource-Limited Growth, Competition, and Predation: A Model and Experimental Studies with Bacteria and Bacteriophage. *The American Naturalist* **111**, 3-24. (doi:10.2307/2459975).

[8] Chao, L., Levin, B.R. & Stewart, F.M. 1977 A Complex Community in a Simple Habitat: An Experimental Study with Bacteria and Phage. *Ecology* **58**, 369-378. (doi:10.2307/1935611).

[9] Lenski, R.E. & Levin, B.R. 1985 Constraints on the coevolution of bacteria and virulent phage: a model, some experiments, and predictions for natural communities. *American Naturalist*, 585-602.

[10] Kerr, B., Neuhauser, C., Bohannan, B.J.M. & Dean, A.M. 2006 Local migration promotes competitive restraint in a host-pathogen 'tragedy of the commons'. *Nature* **442**, 75-78.

[11] Bohannan, B.J. & Lenski, R.E. 2000 The relative importance of competition and predation varies with productivity in a model community. *The American Naturalist* **156**, 329-340.

[12] Forde, S.E., Thompson, J.N. & Bohannan, B.J. 2004 Adaptation varies through space and time in a coevolving host–parasitoid interaction. *Nature* **431**, 841-844.

[13] Brockhurst, M.A., Buckling, A. & Rainey, P.B. 2005 The effect of a bacteriophage on diversification of the opportunistic bacterial pathogen, Pseudomonas aeruginosa. *Proc R Soc B* **272**, 1385-1391. (doi:10.1098/rspb.2005.3086).

[14] Vos, M., Birkett, P.J., Birch, E., Griffiths, R.I. & Buckling, A. 2009 Local Adaptation of Bacteriophages to Their Bacterial Hosts in Soil. *Science* **325**, 833. (doi:10.1126/science.1174173).

[15] Gómez, P. & Buckling, A. 2011 Bacteria-Phage Antagonistic Coevolution in Soil. *Science* **332**, 106-109. (doi:10.1126/science.1198767).

[16] Gomez, P. & Buckling, A. 2013 Coevolution with phages does not influence the evolution of bacterial mutation rates in soil. *ISME J* **7**, 2242-2244. (doi:10.1038/ismej.2013.105).
[17] Koskella, B. & Brockhurst, M.A. 2014 Bacteria–phage coevolution as a driver of ecological and evolutionary processes in microbial communities. *Fems Microbiol Rev* **38**, 916-931. (doi:10.1111/1574-6976.12072).
[18] Persat, A., Nadell, C D., Kim, M K., Ingremeau, F., Siryaporn, A., Drescher, K., Wingreen, N S., Bassler, B L., Gitai, Z. & Stone, H A. 2015 The Mechanical World of Bacteria. *Cell* **161**, 988-997. (doi:http://dx.doi.org/10.1016/j.cell.2015.05.005).
[19] O'Toole, G.A. & Wong, G.C. 2016 Sensational biofilms: surface sensing in bacteria. *Curr Opin Microbiol* **30**, 139-146.
[20] Teschler, J.K., Zamorano-Sanchez, D., Utada, A.S., Warner, C.J.A., Wong, G.C.L., Linington, R.G. & Yildiz, F.H. 2015 Living in the matrix: assembly and control of Vibrio cholerae biofilms. *Nat Rev Micro* **13**, 255-268. (doi:10.1038/nrmicro3433).
[21] Meyer, J.R., Dobias, D.T., Weitz, J.S., Barrick, J.E., Quick, R.T. & Lenski, R.E. 2012 Repeatability and Contingency in the Evolution of a Key Innovation in Phage Lambda. *Science* **335**, 428-432. (doi:10.1126/science.1214449).
[22] Weitz, J.S., Hartman, H. & Levin, S.A. 2005 Coevolutionary arms races between bacteria and bacteriophage. *Proc Natl Acad Sci U S A* **102**, 9535-9540. (doi:10.1073/pnas.0504062102).
[23] van Vliet, S. & Ackermann, M. 2015 Bacterial ventures into multicellularity: collectivism through individuality. *PLoS Biol* **13**, e1002162.
[24] Abedon, S.T. 2008 Bacteriophage Ecology: Population Growth, Evolution, and Impact of Bacterial Viruses. (Cambridge, UK, Cambridge University Press.
[25] Abedon, S.T. 2012 Spatial Vulnerability: Bacterial Arrangements, Microcolonies, and Biofilms as Responses to Low Rather than High Phage Densities. *Viruses-Basel* **4**, 663-687. (doi:10.3390/v4050663).
[26] Nanda, A.M., Thormann, K. & Frunzke, J. 2015 Impact of spontaneous prophage induction on the fitness of bacterial populations and host-microbe interactions. *J Bacteriol* **197**, 410-419.
[27] Koskella, B., Thompson, J.N., Preston, G.M. & Buckling, A. 2011 Local biotic environment shapes the spatial scale of bacteriophage adaptation to bacteria. *The American Naturalist* **177**, 440-451.
[28] Koskella, B. 2013 Phage-mediated selection on microbiota of a long-lived host. *Curr Biol* **23**, 1256-1260.
[29] Díaz-Muñoz, S.L. & Koskella, B. 2014 Bacteria-phage interactions in natural environments. *Adv. Appl. Microbiol* **89**, 10.1016.
[30] Chan, B.K., Abedon, S.T. & Loc-Carrillo, C. 2013 Phage cocktails and the future of phage therapy. *Future Microbiol* **8**, 769-783. (doi:10.2217/fmb.13.47).
[31] Levin, B.R. & Bull, J.J. 2004 Population and evolutionary dynamics of phage therapy. *Nat Rev Microbiol* **2**, 166-173. (doi:10.1038/nrmicro822).
[32] Melo, L.D.R., Sillankorva, S., Ackermann, H.-W., Kropinski, A.M., Azeredo, J. & Cerca, N. 2014 Isolation and characterization of a new Staphylococcus epidermidis broad-spectrum bacteriophage. *Journal of General Virology* **95**, 506-515. (doi:10.1099/vir.0.060590-0).
[33] Pires, D., Sillankorva, S., Faustino, A. & Azeredo, J. 2011 Use of newly isolated phages for control of Pseudomonas aeruginosa PAO1 and ATCC 10145 biofilms. *Research in Microbiology* **162**, 798-806. (doi:10.1016/j.resmic.2011.06.010).

[34] Sillankorva, S., Neubauer, P. & Azeredo, J. 2010 Phage control of dual species biofilms of Pseudomonas fluorescens and Staphylococcus lentus. *Biofouling* **26**, 567-575. (doi:10.1080/08927014.2010.494251).
[35] Azeredo, J. & Sutherland, I.W. 2008 The use of phages for the removal of infectious biofilms. *Current Pharmaceutical Biotechnology* **9**, 261-266. (doi:10.2174/138920108785161604).
[36] Doolittle, M.M., Cooney, J.J. & Caldwell, D.E. 1996 Tracing the interaction of bacteriophage with bacterial biofilms using fluorescent and chromogenic probes. *J Indust Microb* **16**, 331-341. (doi:10.1007/bf01570111).
[37] Briandet, R., Lacroix-Gueu, P., Renault, M., Lecart, S., Meylheuc, T., Bidnenko, E., Steenkeste, K., Bellon-Fontaine, M.N. & Fontaine-Aupart, M.P. 2008 Fluorescence correlation spectroscopy to study diffusion and reaction of bacteriophages inside biofilms. *Appl Environ Microb* **74**, 2135-2143. (doi:10.1128/aem.02304-07).
[38] Lacroix-Gueu, P., Briandet, R., Leveque-Fort, S., Bellon-Fontaine, M.N. & Fontaine-Aupart, M.P. 2005 In situ measurements of viral particles diffusion inside mucoid biofilms. *Comptes Rendus Biologies* **328**, 1065-1072. (doi:10.1016/j.crvi.2005.09.010).
[39] Chan, B.K. & Abedon, S.T. 2015 Bacteriophages and their Enzymes in Biofilm Control. *Curr Pharm Des* **21**, 85-99.
[40] Ackermann, M. 2015 A functional perspective on phenotypic heterogeneity in microorganisms. *Nat Rev Microbiol* **13**, 497-508.
[41] Stewart, P.S. & Franklin, M.J. 2008 Physiological heterogeneity in biofilms. *Nat Rev Microbiol* **6**, 199-210.
[42] Flemming, H.-C. & Wingender, J. 2010 The biofilm matrix. *Nat Rev Microbiol* **8**, 623-633.
[43] Durrett, R. & Levin, S. 1994 The Importance of Being Discrete (and Spatial). *Theoretical Population Biology* **46**, 363-394.
[44] Kovács, Á.T. 2014 Impact of spatial distribution on the development of mutualism in microbes. *Frontiers in Microbiology* **5**, 649. (doi:10.3389/fmicb.2014.00649).
[45] Liu, W.-m., Levin, S.A. & Iwasa, Y. 1986 Influence of nonlinear incidence rates upon the behavior of SIRS epidemiological models. *Journal of mathematical biology* **23**, 187-204.
[46] Scanlan, P.D. & Buckling, A. 2012 Co-evolution with lytic phage selects for the mucoid phenotype of Pseudomonas fluorescens SBW25. *ISME J* **6**, 1148-1158. (doi:10.1038/ismej.2011.174).
[47] Ashby, B., Gupta, S. & Buckling, A. 2014 Spatial Structure Mitigates Fitness Costs in Host-Parasite Coevolution. *The American Naturalist* **183**, E64-E74. (doi:10.1086/674826).
[48] Heilmann, S., Sneppen, K. & Krishna, S. 2012 Coexistence of phage and bacteria on the boundary of self-organized refuges. *P Natl Acad Sci USA* **109**, 12828-12833. (doi:10.1073/pnas.1200771109).
[49] Nadell, C.D., Drescher, K. & Foster, K.R. 2016 Spatial structure, cooperation, and competition in bacterial biofilms. *Nat Rev Microbiol* **14**, 589-600.
[50] Hellweger, F.L., Clegg, R.J., Clark, J.R., Plugge, C.M. & Kreft, J.-U. 2016 Advancing microbial sciences by individual-based modelling. *Nat Rev Microbiol*.
[51] Hellweger, F.L. & Bucci, V. 2009 A bunch of tiny individuals-Individual-based modeling for microbes. *Ecological Modelling* **220**, 8-22. (doi:10.1016/j.ecolmodel.2008.09.004).
[52] Estrela, S., Trisos, C.H. & Brown, S.P. 2012 From metabolism to ecology: cross-feeding interactions shape the balance between polymicrobial conflict and mutualism. *The American naturalist* **180**, 566-576. (doi:10.1086/667887).

582 [53] Estrela, S. & Brown, S.P. 2013 Metabolic and Demographic Feedbacks Shape the
583 Emergent Spatial Structure and Function of Microbial Communities. *PLoS Comput Biol* **9**,
584 e1003398. (doi:10.1371/journal.pcbi.1003398).
585 [54] Naylor, J., Fellermann, H., Ding, Y., Mohammed, W.K., Jakubovics, N.S., Mukherjee, J.,
586 Biggs, C.A., Wright, P.C. & Krasnogor, N. 2017 Simbiotics: a multi-scale integrative
587 platform for 3D modeling of bacterial populations. *ACS Synthetic Biology*.
588 [55] Lardon, L.A., Merkey, B.V., Martins, S., Doetsch, A., Picioreanu, C., Kreft, J.-U. & Smets,
589 B.F. 2011 iDynoMiCS: next-generation individual-based modelling of biofilms. *Environ*
590 *Microbiol* **13**, 2416-2434. (doi:10.1111/j.1462-2920.2011.02414.x).
591 [56] Xavier, J.B., Picioreanu, C. & van Loosdrecht, M.C.M. 2005 A framework for
592 multidimensional modelling of activity and structure of multispecies biofilms. *Environ*
593 *Microbiol* **7**, 1085-1103. (doi:10.1111/j.1462-2920.2005.00787.x).
594 [57] Bucci, V., Nadell, C.D. & Xavier, J.B. 2011 The evolution of bacteriocin production in
595 bacterial biofilms. *American Naturalist* **178**, E162-E173.
596 [58] Alpkvist, E. & Klapper, I. 2007 Description of mechanical response including
597 detachment using a novel particle model of biofilm/flow interaction. *Water Sci Technol*
598 **55**, 265-273.
599 [59] Chambless, J.D. & Stewart, P.S. 2007 A three-dimensional computer model analysis of
600 three hypothetical biofilm detachment mechanisms. *Biotechnol Bioeng* **97**, 1573-1584.
601 [60] Stewart, P.S. 2012 Mini-review: Convection around biofilms. *Biofouling* **28**, 187-198.
602 (doi:10.1080/08927014.2012.662641).
603 [61] Drescher, K., Shen, Y., Bassler, B.L. & Stone, H.A. 2013 Biofilm streamers cause
604 catastrophic disruption of flow with consequences for environmental and medical
605 systems. *Proceedings of the National Academy of Sciences* **110**, 4345-4350.
606 (doi:10.1073/pnas.1300321110).
607 [62] Bohn, A., Zippel, B., Almeida, J.S. & Xavier, J.B. 2007 Stochastic modeling for
608 characterisation of biofilm development with discrete detachment events (sloughing).
609 *Water Science and Technology* **55**, 257-264. (doi:10.2166/wst.2007.266).
610 [63] Xavier, J.B., Picioreanu, C. & Van Loosdrecht, M.C.M. 2004 A modelling study of the
611 activity and structure of biofilms in biological reactors. *Biofilms* **1**, 377-391.
612 [64] Xavier, J.B., Picioreanu, C., Rani, S.A., van Loosdrecht, M.C.M. & Stewart, P.S. 2005
613 Biofilm-control strategies based on enzymic disruption of the extracellular polymeric
614 substance matrix - a modelling study. *Microbiology-Sgm* **151**, 3817-3832.
615 (doi:10.1099/mic.0.28165-0).
616 [65] Xavier, J.B., Picioreanu, C. & van Loosdrecht, M. 2005 A general description of
617 detachment for multidimensional modelling of biofilms. *Biotechnology and*
618 *Bioengineering* **91**, 651-669.
619 [66] McCrea, W. & Whipple, F. 1940 Random Paths in Two and Three Dimensions.
620 *Proceedings of the Royal Society of Edinburgh* **60**, 281-298.
621 [67] Motwani, R. & Raghavan, P. 1995 *Randomized Algorithms*. Cambridge, UK, Cambridge
622 University Press.
623 [68] N, B., L, O. & J, S. 2013 PyAMG: Algebraic Multigrid Solvers in Python. (
624 [69] Bresenham, J.E. 1965 Algorithm for computer control of a digital plotter. *IBM*
625 *Systems journal* **4**, 25-30.
626 [70] Dijkstra, E.W. 1959 A note on two problems in connexion with graphs. *Numerische*
627 *mathematik* **1**, 269-271.
628 [71] Xavier, J.d.B., Picioreanu, C. & van Loosdrecht, M.C.M. 2005 A general description of
629 detachment for multidimensional modelling of biofilms. *Biotechnology and bioengineering*
630 **91**, 651-669.

[72] Nadell, C.D., Bucci, V., Drescher, K., Levin, S.A., Bassler, B.L. & Xavier, J.B. 2013 Cutting through the complexity of cell collectives. *Proc R Soc B* **280**, 20122770.
[73] Heilmann, S., Sneppen, K. & Krishna, S. 2010 Sustainability of virulence in a phage-bacterial ecosystem. *Journal of virology* **84**, 3016-3022.
[74] Nadell, C.D., Foster, K.R. & Xavier, J.B. 2010 Emergence of spatial structure in cell groups and the evolution of cooperation. *PLoS Comput Biol* **6**, e1000716.
[75] Mitri, S., Clarke, E. & Foster, K.R. 2015 Resource limitation drives spatial organization in microbial groups. *ISME J.* (doi:10.1038/ismej.2015.208).
[76] Picioreanu, C., van Loosdrecht, M.C.M. & Heijnen, J.J. 1998 Mathematical modeling of biofilm structure with a hybrid differential-discrete cellular automaton approach. *Biotechnology and Bioengineering* **58**, 101-116.
[77] Endy, D., You, L., Yin, J. & Molineux, I.J. 2000 Computation, prediction, and experimental tests of fitness for bacteriophage T7 mutants with permuted genomes. *Proceedings of the National Academy of Sciences* **97**, 5375-5380. (doi:10.1073/pnas.090101397).
[78] Abedon, S.T. 2015 Ecology of anti-biofilm agents ii: bacteriophage exploitation and biocontrol of Biofilm Bacteria. *Pharmaceuticals* **8**, 559-589.
[79] Keeling, M.J. 1999 The effects of local spatial structure on epidemiological invasions. *Proceedings of the Royal Society of London B: Biological Sciences* **266**, 859-867.
[80] Balcan, D., Colizza, V., Gonçalves, B., Hu, H., Ramasco, J.J. & Vespignani, A. 2009 Multiscale mobility networks and the spatial spreading of infectious diseases. *Proceedings of the National Academy of Sciences* **106**, 21484-21489.
[81] Riley, S. 2007 Large-scale spatial-transmission models of infectious disease. *Science* **316**, 1298-1301.
[82] May, R.M. & Anderson, R.M. 1979 Population biology of infectious diseases: Part II. *Nature* **280**, 455-461.
[83] Holt, R.D., Dobson, A.P., Begon, M., Bowers, R.G. & Schauber, E.M. 2003 Parasite establishment in host communities. *Ecology Letters* **6**, 837-842.
[84] Lloyd-Smith, J.O., Cross, P.C., Briggs, C.J., Daugherty, M., Getz, W.M., Latto, J., Sanchez, M.S., Smith, A.B. & Swei, A. 2005 Should we expect population thresholds for wildlife disease? *Trends in Ecology & Evolution* **20**, 511-519.
[85] Webb, S.D., Keeling, M.J. & Boots, M. 2007 Host–parasite interactions between the local and the mean-field: How and when does spatial population structure matter? *J. Theo. Biol.* **249**, 140-152.
[86] Boots, M. & Sasaki, A. 2002 Parasite ‐ driven extinction in spatially explicit host ‐ parasite systems. *The American Naturalist* **159**, 706-713.
[87] Rand, D., Keeling, M. & Wilson, H. 1995 Invasion, stability and evolution to criticality in spatially extended, artificial host-pathogen ecologies. *Proceedings of the Royal Society of London B: Biological Sciences* **259**, 55-63.
[88] Satō, K., Matsuda, H. & Sasaki, A. 1994 Pathogen invasion and host extinction in lattice structured populations. *Journal of mathematical biology* **32**, 251-268.
[89] Levin, S.A. 1992 The Problem of Pattern and Scale in Ecology: The Robert H. MacArthur Award Lecture. *Ecology* **73**, 1943-1967. (doi:10.2307/1941447).
[90] Flemming, H.-C., Wingender, J., Szewzyk, U., Steinberg, P., Rice, S.A. & Kjelleberg, S. 2016 Biofilms: an emergent form of bacterial life. *Nat Rev Microbiol* **14**, 563-575.
[91] Nadell, C.D., Drescher, K., Wingreen, N.S. & Bassler, B.L. 2015 Extracellular matrix structure governs invasion resistance in bacterial biofilms. *ISME J* **9**, 1700-1709. (doi:10.1038/ismej.2014.246).
[92] Nadell, C.D., Xavier, J.B. & Foster, K.R. 2009 The sociobiology of biofilms. *Fems Microbiol Rev* **33**, 206-224. (doi:DOI 10.1111/j.1574-6976.2008.00150.x).

[93] Branda, S.S., Vik, S., Friedman, L. & Kolter, R. 2005 Biofilms: the matrix revisited. *Trends Microbiol* **13**, 20-26.
[94] Dragoš, A. & Kovács, Á.T. 2017 The Peculiar Functions of the Bacterial Extracellular Matrix. *Trends Microbiol*.
[95] Abedon, S. 2017 Phage "delay" toward enhancing bacterial escape from biofilms: a more comprehensive way of viewing resistance to bacteriophages. *AIMS Microbiology* **3**, 186-226.
[96] Sutherland, I.W., Hughes, K.A., Skillman, L.C. & Tait, K. 2004 The interaction of phage and biofilms. *Fems Microbiol Lett* **232**, 1-6. (doi:10.1016/s0378-1097(04)00041-2).
[97] Davies, E.V., James, C.E., Williams, D., O'Brien, S., Fothergill, J.L., Haldenby, S., Paterson, S., Winstanley, C. & Brockhurst, M.A. 2016 Temperate phages both mediate and drive adaptive evolution in pathogen biofilms. *Proceedings of the National Academy of Sciences* **113**, 8266-8271. (doi:10.1073/pnas.1520056113).
[98] McCarty, P.L. 2012 *Environmental biotechnology: principles and applications*, Tata McGraw-Hill Education.
[99] Stewart, P. 2003 Diffusion in Biofilms. *J. Bacteriol.* **185**, 1485-1491.
[100] Henze, M., Grady Jr, C., Gujer, W., Marais, G. & Matsuo, T. 1987 Activated sludge model no. 1: Iawprc scientific and technical report no. 1. *IAWPRC, London*.
[101] Loferer-Krößbacher, M., Klima, J. & Psenner, R. 1998 Determination of Bacterial Cell Dry Mass by Transmission Electron Microscopy and Densitometric Image Analysis. *Appl Environ Microb* **64**, 688-694.
[102] Laspidou, C.S. & Rittmann, B.E. 2004 Modeling the development of biofilm density including active bacteria, inert biomass, and extracellular polymeric substances. *Water Res* **38**, 3349-3361.
[103] Delbrück, M. 1945 The burst size distribution in the growth of bacterial viruses (bacteriophages). *J Bacteriol* **50**, 131.
[104] Cairns, B.J., Timms, A.R., Jansen, V.A., Connerton, I.F. & Payne, R.J. 2009 Quantitative models of in vitro bacteriophage–host dynamics and their application to phage therapy. *PLoS Pathog* **5**, e1000253.

717 **Table 1: Model Parameters used for Simulations**
718

Parameter	Value used in the simulations	Description	References
x_{max}, y_{max}	$1000um, 1000um$	The physical size of the system	N/A
dl, dV	$4\ um, 64\ um^3$	Length and volume of a grid element	N/A
N_{max}	$5 - 1200\ mg\ L^{-1}$	Maximum density of substrate (spanned along during simulations)	[98]
D_N	$6.944 * 10^{-6}$ $cm^2\ s^{-1}$	Substrate diffusivity	[99]
K_N	$4\ mg\ L^{-1}$	Half saturation constant for substrate	[56, 100]
δ_E	$1.417\ (m\ h)^{-1}$	Erosion constant	[65]
m_s	$10^{-12} g$	Bacterial mass per cell	[101]
δ_d	$0.0792\ day^{-1}$	Decay to inert mass constant	[100]
μ_s	$28.5\ day^{-1}$	Maximum growth rate	[65]
I_{max}	$1000\ g\ L^{-1}$	Maximum inert biomass density	[102]
S_{max}	$200\ g\ L^{-1}$	Maximum active biomass density	[102]
Y	0.495	Yield of substrate converted to biomass	[57]
β	100	Phage burst size	[24, 77, 103]
D_P	$2.08 * 10^{-7}$ $cm^2\ s^{-1}$	Phage diffusivity constant	[24]
Z_P	$1 - 18$	Phage Impedance	This Study
δ_{pd}	$0.2083\ h^{-1}$	Phage decay constant	[104]
τ	$28.8\ minutes$	Incubation period before lysis	[24]
γ	$0.021 - 9.59\ h^{-1}$	Infection rate per biomass per phage	This Study (scaled to model infection probability of .1-99% per host encounter

719
720

Figure Legends

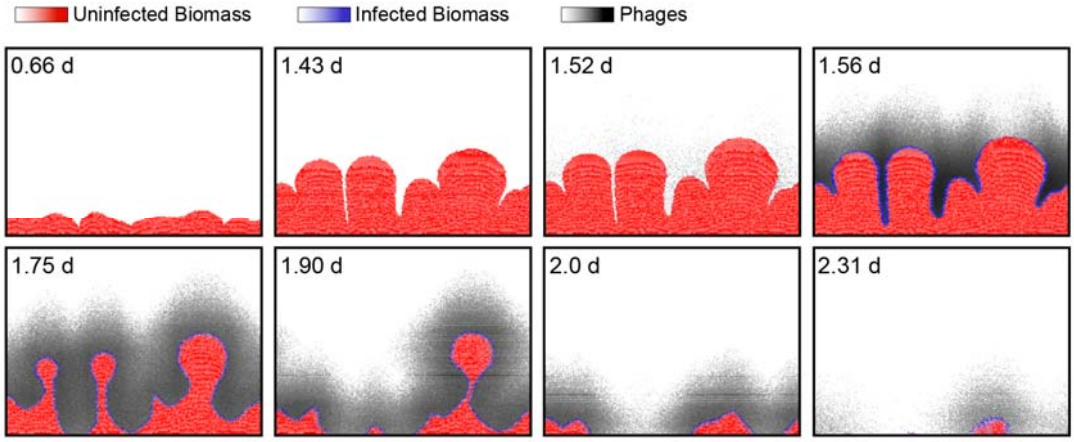

Figure 1. An example time series of simulated biofilm growth and phage infection. For uninfected and infected biomass (red and blue, respectively), the color gradients are scaled to the maximum permissible biomass per grid node (see Supplemental Methods). For phages, the black color gradient is scaled to the maximum phage concentration in this run of the simulation. Any phages that diffuse away from the biofilm into the surrounding liquid are assumed to be advected out of the system in the next iteration cycle. Phages are introduced to the biofilm at 1.5 d. Phage infection proliferates along the biofilm front, causing biomass erosion and, in this example, complete eradication of the biofilm population. The simulation space is 250 μm long along its horizontal dimension.

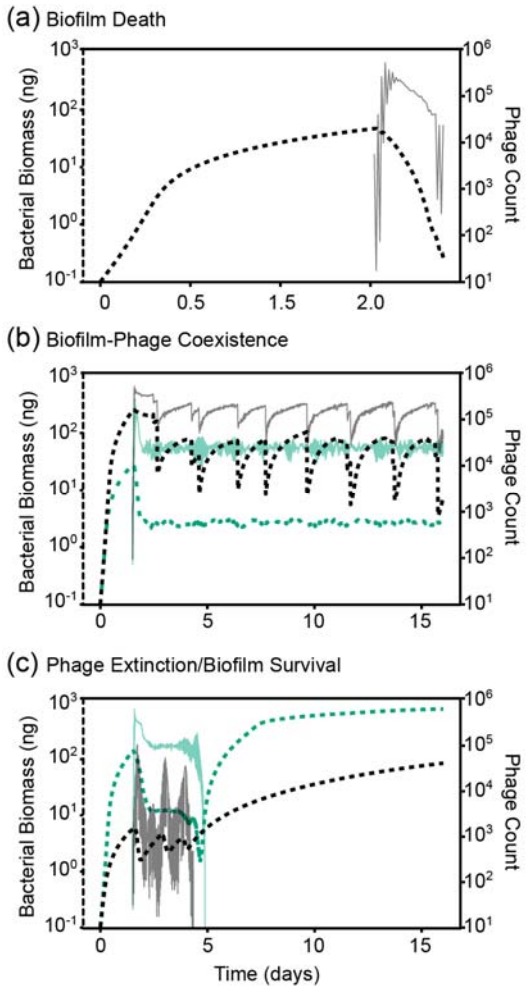

Figure 2. Population dynamics of biofilm-dwelling bacteria and phages for several example cases. For each example simulation, bacterial biomass is plotted in the thick dotted line (left axis), and phage counts are plotted in the thin solid line (right axis) (a) Biofilm death: phages rapidly proliferate and bacterial growth cannot compensate, resulting in clearance of the biofilm population (and halted phage proliferation thereafter). (b) Coexistence of bacteria and phages. We found two broad patterns of coexistence, one in which bacteria and phage populations remained at relative fixed population size (green lines), and one in which bacterial and phage populations oscillated as large biofilms clusters grew, sloughed, and re-grew repeatedly over time (black lines). (c) Phage extinction and biofilm survival. In many cases we found that phage populations extinguished while biofilms were relatively small, allowing the small population of remaining bacteria to grow unobstructed thereafter. Some of these cases involved phage population oscillations of large amplitude (black lines), while others did not (green lines).

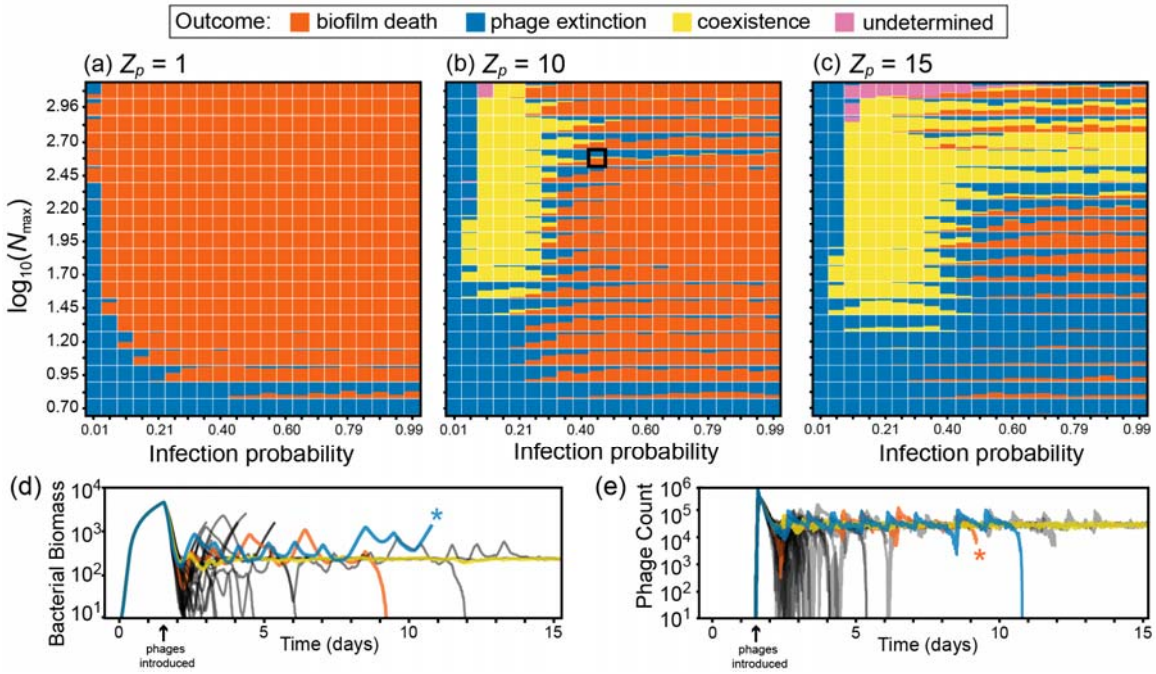

Figure 3. Steady states of biofilm-phage population dynamics as a function of nutrient availability, phage infection rate, and phage impedance. Each point in each heatmap summarizes >30 simulation runs, and shows the distribution of simulation outcomes. Phage extinction (biofilm survival) is denoted by blue, biofilm-phage coexistence is denoted by yellow, and biofilm death is denoted by orange. Each map is a parameter sweep of nutrient availability (~biofilm growth rate) on the vertical axis, and infection probability per phage-bacterium contact event on the horizontal axis. The sweep was performed for three values of *Zp*, the phage impedance, where phage diffusivity within biofilm biofilms is equivalent to that in liquid for *Zp* = 1 (panel a), and decreases with increasing *Zp* (panels b and c). For *Zp* = [10,15], there are regions of stable coexistence (all-yellow points) and unstable coexistence (bi- and tri-modal points) between phages and bacteria. Traces of (d) bacterial biomass and (e) phage count are provided for one parameter combination at *Zp* = 10 (identified with a black box in panel b) corresponding to unstable phage-bacterial coexistence. We have highlighted one example each of phage extinction (blue), biofilm death (orange), and coexistence (yellow), which in this case is likely transient. In the highlighted traces, asterisks denote that the simulations were stopped because either phages or the bacterial biomass had declined to zero. This was done to increase the overall speed of the parallelized simulation framework. Simulations were designated "undetermined" if biofilms reached the ceiling of the simulation space before any of the other outcomes occurred (see main text).

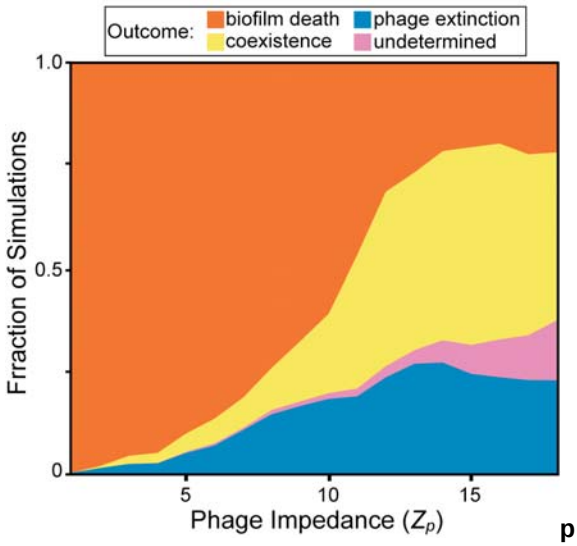

p

Figure 4. The distribution of biofilm-phage population dynamic steady states as a function of increasing phage mobility impedance within the biofilm. Here we performed sweeps of nutrient and infection probability parameter space for values of phage impedance (Z_P) ranging from 1-18. As the phage impedance parameter is increased, phage diffusion within the biofilm becomes slower relative to the surrounding liquid phase. The replication coverage was at least 6 runs for each combination of nutrient concentration, infection probability, and phage impedance, totaling 96,000 simulations. Undetermined simulations are those in which biofilms reached the simulation height maximum before any of the other exit conditions occurred (see main text).